ACS APPLIED MATERIALS & INTERFACES

Research Article

www.acsami.org

Optically Transparent Superhydrophobic Surfaces with Enhanced Mechanical Abrasion Resistance Enabled by Mesh Structure

Naoyuki Yokoi, Kengo Manabe, Mizuki Tenjimbayashi, and Seimei Shiratori*

School of Integrated Design Engineering, Keio University, 3-14-1 Hiyoshi, Kohoku-ku, Yokohama-shi, Kanagawa-ken 223-8522, Japan

Supporting Information

ABSTRACT: Inspired by naturally occurring superhydrophobic surfaces such as "lotus leaves", a number of approaches have been attempted to create specific surfaces having nano/microscale rough structures and a low surface free energy. Most importantly, much attention has been paid in recent years to the improvement of the durability of highly transparent superhydrophobic surfaces. In this report, superhydrophobic surfaces are fabricated using three steps. First, chemical and morphological changes are generated in the polyester mesh by alkaline treatment of NaOH. Second, alkaline treatment causes hydrophobic molecules of 1*H*,1*H*,2*H*,2*H*-perfluorodecyltrichlorosilane to react with the hydroxyl groups on the fiber surfaces forming covalent bonds by using the chemical vapor deposition method. Third, hydrophobicity is enhanced by treating the mesh with SiO_2 nanoparticles modified with 1*H*,1*H*,2*H*,2*H*-perfluorooctyltriethoxysilane using a spray method. The transmittance of the fabricated superhydrophobic mesh is approximately 80% in the spectral range of 400−1000 nm. The water contact angle and the water sliding angle remain greater than 150° and lower than 25°, respectively, and the transmittance remains approximately 79% after 100 cycles of abrasion under approximately 10 kPa of pressure. The mesh surface exhibits a good resistance to acidic and basic solutions over a wide range of pH values (pH 2−14), and the surface can also be used as an oil/water separation material because of its mesh structure.

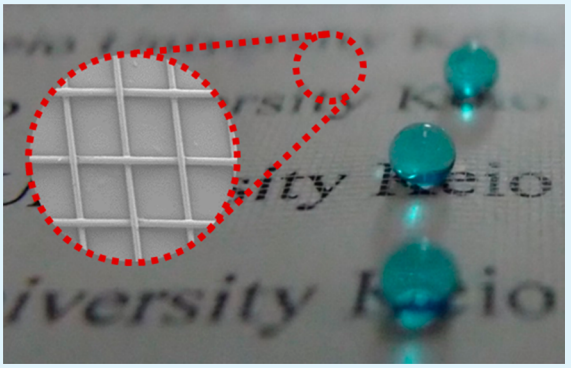

KEYWORDS: *superhydrophobic surfaces, transparency, mechanical durability, polyester mesh, oil/water separation*

INTRODUCTION

In nature, the surfaces of many plant leaves,[1−3] insect legs,[4,5] hairs,[6] and wings,[7] and animal fur and feathers show extremely high water repellency, wherein the water contact angle (WCA) of the surfaces is over 150° with small water sliding angles (WSA). Such surfaces are often referred to as superhydrophobic. Generally, wetting behavior is dependent upon both the surface chemistry and the surface topography,[8,9] and the presence of hierarchical roughness such as that found in lotus leaves further increases the contact angle by creating more trapped air pockets on the surfaces and lowers the WSAs.[10] Therefore, the combination of micro- and nanoscale roughness increases the contact angle of water such that water droplets cannot adhere but are forced to roll off.[11] Providing proper roughness is an important requirement for the processing of superhydrophobic surfaces, and numerous methods to fabricate the surfaces have been reported.[12−19] Because of their characteristics, superhydrophobic surfaces have numerous applications in self-cleaning windows and paints,[20] nonwetting fabrics,[21−23] antifogging,[24] anti-icing,[25−27] buoyancy,[28] and flow enhancement.[29]

For practical applications, it is important that the coating is mechanically durable against wear, shear, and ice adhesion. Mechanical robustness is particularly critical because the nanoscale roughness can easily be destroyed irreversibly, leading to a rapid decrease of the WCA and an increase of the WSA.[30] Several methods have been proposed to improve the durability of superhydrophobic surfaces, including enhancement of mechanical stability,[31−33] improvement of corrosion resistance,[34] self-healing of topographic structures, and self-repairing of surface chemical properties.[35−37] It is also important that the superhydrophobic surfaces are transparent to expand the range of possible applications. Recently, increasing interest in energy efficiency has promoted research in developing coatings that are both self-cleaning and transparent.[38−42] In general, however, surface roughness and transparency are competitive properties because surface roughness, although a prerequisite for fabricating superhydrophobic surfaces, may also lead to opacity because of increased light scattering. Light scattering is a function of roughness size and the refractive index of the materials, so careful control of the roughness and matching the refractive index of the coating materials with that of the substrate are important to prevent light scattering and to fabricate both high transparency and superhydrophobic surfaces. For the practical applications of transparent superhydrophobic surfaces, it is

Received: December 10, 2014
Accepted: January 27, 2015
Published: January 27, 2015

DOI: 10.1021/am508726k
ACS Appl. Mater. Interfaces 2015, 7, 4809−4816

critical that they possess long-term durability of the self-assembled nanostructures against mechanical wear, shear, and liquid flow. However, it is especially challenging to improve the abrasion resistance of the highly transparent superhydrophobic surfaces because, in general, if there is no chemical or physical bonding between the particles or the particles and the substrate, the coating can be easily removed by Scotch tape peeling. In addition to Scotch tape peeling and the tribology wear test, waterfall/jet and sand abrasion tests have often been used to evaluate the robustness of the transparent superhydrophobic coating, where changes in the WCA and WSA and in the coating morphology before and after the tests are compared. Generally, abrasion tests have often been used to evaluate the robustness of superhydrophobic and superoleophobic coatings; however, few abrasion tests have been reported on transparent superhydrophobic coatings. Yanagisawa et al. designed superhydrophobic surfaces based on a surface microstructure combination on a rigid base film with craterlike hemispherical holes and acicular nanoparticles, where the WCA of the coating was 163 ± 1° and the transparency was approximately 85% before rubbing abrasion. After two rubbing abrasion cycles, the WCA of these surfaces was under 150° and further decreased to approximately 127° after 30 cycles of rubbing abrasion.[43]

Clearly, the superhydrophobic coatings must be easy to fabricate, transparent, and mechanically resistant and must exhibit long-term stability, and, to date, none of the existing methods or coatings developed have fulfilled all of these requirements. We have been investigating a method for superhydrophobic surface fabrication to produce surfaces with high transparency and increased mechanical durability against wear and abrasion resistance, selecting the strategy of using the see-through structures of polyester mesh.[44] Fabrics and meshes have been used as substrates in many previous studies of superhydrophobic thin films.[44−46] For example, fabric-based superhydrophobic and superoleophilic thin films have been used as oil/water filters.[47−52] In our previous study, we designed a mesh-based superoleophobic surface with SiO_2 nanoparticles. Although the contact angles of hexadecane and water droplets were over 150° and the transparency was approximately 61%, the high durability of the film has not been achieved due to exposure of native mesh surfaces by removing the SiO_2 nanoparticles after abrasion.[44] Therefore, the maintaining superhydrophobicity of the surface after abrasion can be improved by two approaches; one is developing the surface structures to protect the SiO_2 nanoparticles against the abrasion. The other is that the mesh surface with low surface energy should appear and keep superhydrophobic property in the case that the SiO_2 nanoparticles are removed by the abrasion. To the best of our knowledge, however, no studies have reported the possibility of a mesh-based highly transparent and superhydrophobic thin film with enhanced mechanical abrasion resistance. A mesh structure has four important roles: the vacant space between the fibers of the fabric allows the penetration of visible light and traps an air layer to realize the Cassie state, which is very important for producing superhydrophobicity. Because the transparency of the mesh is due to the penetration of visible light between the fibers, it is unnecessary to control roughness or to carefully match the refractive index of the coating materials with that of the substrate. However, the microroughness of the three-dimensional microstructure of the meshes should be optimized to improve its mechanical stability and to maintain and protect the nanoroughness provided by the SiO_2 nanoparticles. Finally, the fabrics have high flexibility. For these surfaces, we react 1*H*,1*H*,2*H*,2*H*-perfluorodecyltrichlorosilane (PFDTS) at the fibers of the fabric as a precaution against the removal of the SiO_2 nanoparticles modified with 1*H*,1*H*,2*H*,2*H*-perfluorooctyltriethoxysilane (PFOTS) at the mesh surfaces. In this way, even if the hydrophobic SiO_2 nanoparticles are removed by abrasion, the mesh surfaces treated with PFDTS maintain a low surface energy property and retain their superhydrophobicity.

In this paper, we investigate the possibility of a highly transparent and superhydrophobic thin film with enhanced mechanical abrasion resistance by combining a see-through hydrophobic mesh with a hydrophobic SiO_2 nanoparticle hierarchical structure. This simple but novel and effective method may be useful for the improvement of highly transparent superhydrophobic surfaces for various applications.

EXPERIMENTAL SECTION

Materials. Polyester fabrics supplied by Clever Co., Ltd. (Toyohashi, Japan) were used as a substrate, possessing fiber diameters of 55 μm, a fiber separation distance of 370 μm, and a transmittance of approximately 75%. The SiO_2 nanoparticles with an average primary particle diameter of 40 nm were obtained from Nippon AEROSIL Co., Ltd. (Tokyo, Japan). The 1*H*,1*H*,2*H*,2*H*-perfluorodecyltrichlorosilane (PFDTS) was obtained from Tokyo Chemical Industry Co., Ltd. (Tokyo, Japan), the 1*H*,1*H*,2*H*,2*H*-perfluorooctyltriethoxysilane (PFOTS) was obtained from Gelest, Inc. (United States), and the tetraethoxysilane (TEOS) was obtained from Wako Pure Chemical Industries, Ltd. (Osaka, Japan). Distilled water, with an interfacial tension of liquid vapor of γlv = 72.8 mN m^{-1}, was used as a solvent and also as a probe liquid to evaluate the WCAs and WSAs. To prove the repellency against any pH solution, acidic and basic aqueous solutions were prepared by adding hydrochloric acid and NaOH, respectively. Hydrochloric acid and NaOH were obtained from Kanto Chemical Co., Inc. (Tokyo, Japan).

Fabrication of Highly Transparent Robust Superhydrophobic Mesh Film. The original mesh films used as substrates were rinsed sequentially with deionized water and ethanol and then dried at room temperature. The superhydrophobic surfaces were fabricated using the three steps, including the coating procedure, presented schematically in Figure 1. First, chemical and morphological changes

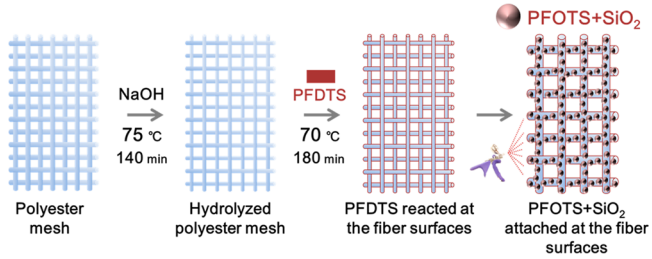

Figure 1. Schematic of the fabrication procedure for the superhydrophobic polyester mesh. First, a polyester mesh undergoes an alkaline treatment with NaOH. Second, PFDTS is reacted on the fiber surfaces using the chemical vapor deposition method. Third, the mesh is treated with SiO_2 nanoparticles modified with PFOTS using a spray method.

were generated in the polyester mesh by an alkaline treatment with NaOH. The prepared mesh was then immersed in a 200 g/L sodium hydroxide solution, whereupon the solution was heated to 75 °C for 140 min and the soaked meshes were subsequently washed with abundant deionized water and dried at room temperature.[53] Second, hydrophobic molecules of PFDTS were reacted with the hydroxyl groups existing on the fiber surfaces caused by the alkaline treatment, forming covalent bonds by using the chemical vapor deposition method. The meshes were placed in a 100 mL sealed vessel along with

DOI: 10.1021/am508726k
ACS Appl. Mater. Interfaces 2015, 7, 4809−4816

a container filled with 0.2 mL of PFDTS with no direct contact between the liquid and the meshes, whereupon the vessel was heated to 70 °C for 180 min and then cooled to room temperature.[54] These steps made the obtained hydrophobic textiles durable against strong abrasion. Third, to enhance the hydrophobicity, the meshes were treated with SiO_2 nanoparticles modified with PFOTS using a spray method. The amount of 0.38 mg of SiO_2 nanoparticles was added to 35.08 mg of acetone and stirred for 5 min, after which 0.80 mg of TEOS and 0.45 mg of PFOTS were added to the solution and stirred for 5 min, whereupon 0.09 mg of hydrochloric acid and 0.76 mg of deionized water were added. Acetone, PFOTS, and hydrochloric acid are used as a solvent, a lower energy material, and catalyst, respectively. TEOS is used for bonding between the particles or the particles and the substrate in order to enhance the durability. After stirring for 30 min, the solution was sprayed on the meshes using a spray gun (nozzle diameter: 0.6 mm, XP7; Airtex Co., Ltd., Tokyo, Japan), and the meshes were subsequently dried at room temperature.[44,55] The spraying pressure of a spray gun was 0.6 MPa, the amount of the sprayed solution was 0.3 mL/cm^2, and the spraying distance between spray gun and substrate was 30 cm.

Characterization. A commercial contact angle system (FACE; Kyowa Interface Science Co., Ltd., Niiza, Japan) was used to measure the WCAs and WSAs of the thin films at room temperature, wherein water was used as probe liquid. The reported WCAs and WSAs in this report are the averages of measurements obtained at five different points on each sample surface, with each static contact angle measurement performed using liquid droplets 10 μL in volume. The morphological characterization of the samples was examined using a field emission scanning electron microscope (FE-SEM, S4700; Hitachi, Japan), where all samples were coated with osmium before observation. The transmittance of the obtained fabrics was measured using a spectrophotometer (UVmini-1240; Shimadzu, Kyoto, Japan). The chemical composition of the surface was measured by X-ray photoelectron spectroscopy (XPS, JPS-9010TR; JEOL Ltd., Akishima, Japan), and the surface mechanical durability was observed using an abrasion device (Tribogear Type 18 L; Shinto Scientific Co., Ltd., Tokyo, Japan), where cellulose fibers (cotton) were used as the abrasive material.

RESULTS AND DISCUSSION

Mesh Morphology. The FE-SEM images of pristine polyester meshes (Figure 2a and 2d) demonstrate that the original fibers are smooth and the diameters of the fibers can be estimated to be 55 ± 1 μm, with the distance between the fibers approximately 370 ± 2 μm. However, FE-SEM images of the meshes after alkaline treatment with NaOH (Figures 2b, 2e, and Supporting Information S1) reveal that pits are formed on the fiber surfaces, which appear to be in locations identified as having lower crystallinity,[56] while the fiber diameters are estimated as 45 ± 1 μm and the distance between the fibers is approximately 378 ± 2 μm. Figure 2c and 2f displays a large area of the meshes covered with hydrophobic SiO_2 nanoparticles, where the spray coating covers the polyester meshes uniformly, providing a roughness at the nanoscale to complement the microscale roughness inherent in the mesh weave. This resulting hierarchical roughness at the nanoscale and the microscale formed in the coated fabric is well-known to enhance liquid repellency.

Wetting Characteristic of the Fabricated Mesh. The native meshes are all superhydrophilic, where water droplets can completely wet the mesh surfaces and, additionally, the meshes after alkaline treatment with NaOH are also superhydrophilic. However, the surface fluorination process turns the surfaces of the mesh hydrophobic, though the surfaces exhibit high WSAs before and after abrasion. The meshes treated with SiO_2 nanoparticles modified with PFOTS using a spray method

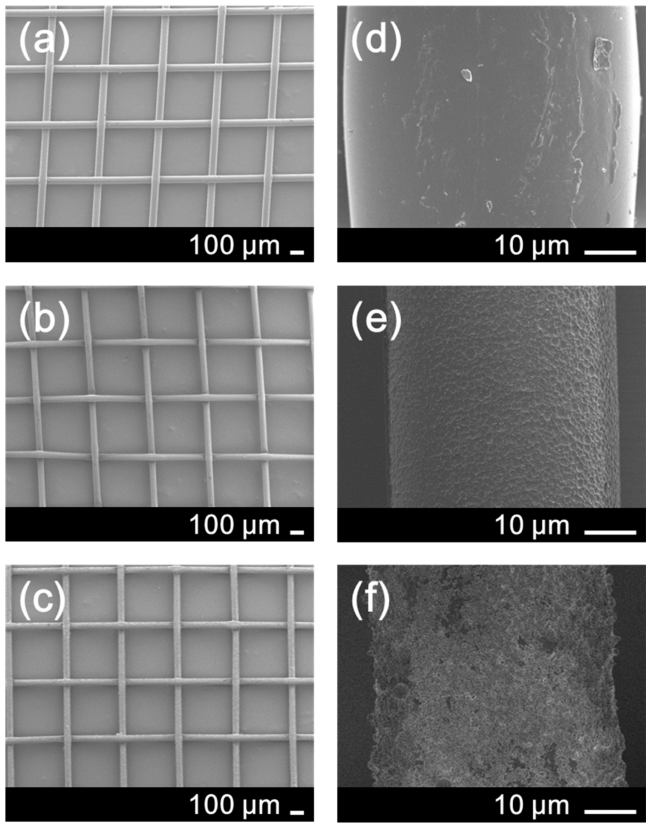

Figure 2. FE-SEM images of (a) pristine polyester meshes, (b) polyester meshes after alkaline treatment with NaOH, and (c) polyester meshes after spray coating with nanoparticles. (d, e, and f) Higher magnification images of the fibers in (a), (b), and (c), respectively.

are found to be superhydrophobic, and the surfaces exhibit a lower WSA than that of the mesh prior to the nanoparticle coating, as listed in Table 1.

Table 1. Water Contact Angles and Sliding Angles before and after Spray Coating with SiO_2 Nanoparticles Modified with PFOTS

	contact angle (deg)	sliding angle (deg)
before spray coating	147.2 ± 3.3	38.9 ± 9.7
after spray coating	153.2 ± 2.5	11.1 ± 2.5

Mechanical stability is important for practical application of the transparent superhydrophobic coatings, so the abrasion durabilities of the coated meshes are evaluated. The methodology of the abrasion test is illustrated in Figure 3, wherein cellulose textiles serve as an abrasion surface and the superhydrophobic meshes to be tested face this abrasion material. With a load pressure of ∼10 kPa applied to the mesh, the cotton is moved back and forth with a speed of 10 mm/s.

The variation in the values of both the WCA and WSA on the coated mesh after an increasing number of abrasion cycles is shown in Figure 4, where it can be seen that, after 100 cycles of abrasion, the WCA of the coated mesh decreases to 152° and the WCA value undergoes a slight change with the number of abrasion cycles. Although the WSA increases with the number of abrasion cycles, it is still lower than 25° after the mesh is subjected to 100 cycles of abrasion. Water droplets still maintain a spherical shape on the superhydrophobic meshes

DOI: 10.1021/am508726k
ACS Appl. Mater. Interfaces 2015, 7, 4809−4816

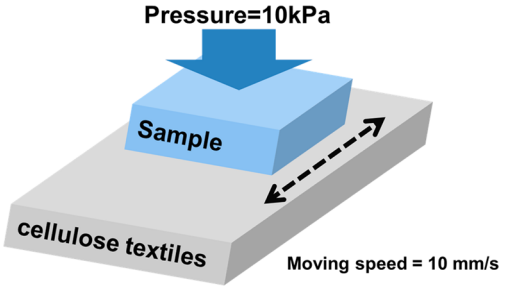

Figure 3. Schematic of the abrasion test employed to evaluate the mechanical durability of the coated meshes.

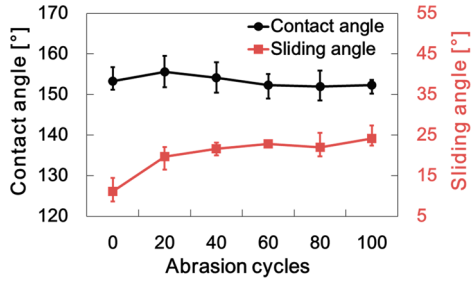

Figure 4. Water contact angle and sliding angle of the superhydrophobic surface as a function of abrasion cycles with a pressure of ~10 kPa.

before and after 100 cycles of abrasion and can easily roll off at a small WSA. These results indicate that the coated meshes can withstand 100 abrasion cycles without a significant reduction in its superhydrophobicity. The WCAs for water droplets placed on the coated surfaces vary from 153° in the initial state to 152° after 100 cycles of abrasion, whereas the WSA has a range of 11−24°. It is found that the rough surface texture of the mesh is retained after abrasion, which is essential for the robust superhydrophobicity of the mesh. However, the WSA increases to 24°, which can be ascribed to a partial loss of the surface roughness and the removal of PFOTS-modified SiO_2 nanoparticles at the mesh surfaces. Observation using FE-SEM (Figure 5) reveals that the coating of PFOTS-modified SiO_2 nanoparticles is mostly retained on the mesh, with only those areas exposed to the abrasive forces (white dotted frame in Figure 5b) exhibiting signs of damage, and the majority of the nanoparticles protected by the three-dimensional microstructure of the mesh. Because the postabrasion residual layer also remains hydrophobic, the overall superhydrophobic properties of the mesh are retained. It is generally assumed that the relative robustness of the superhydrophobicity of the lotus leaf is owing to its two-tier roughness. Indeed, even if more particles are removed in these meshes, the overall superhydrophobic properties remain because the PFDTS-treated polyester surfaces are not hydrophilic but hydrophobic and, therefore, the meshes after 100 cycles of abrasion do not exhibit a high WSA, as listed in Table 2.

The XPS measurements investigate the chemical condition of the surfaces with and without PFDTS treatment after 100 cycles of abrasion. Figure 6 shows the survey spectra and the C 1s core level spectra of the polyester surfaces with and without PFDTS treatment postabrasion, which clearly reveals the presence of elements such as C, O, F, and Si. Table 3 shows the atomic percentage measured by XPS on the polyester surfaces with and without PFDTS treatment postabrasion. Figure 6b and 6c shows the higher resolution C 1s core level

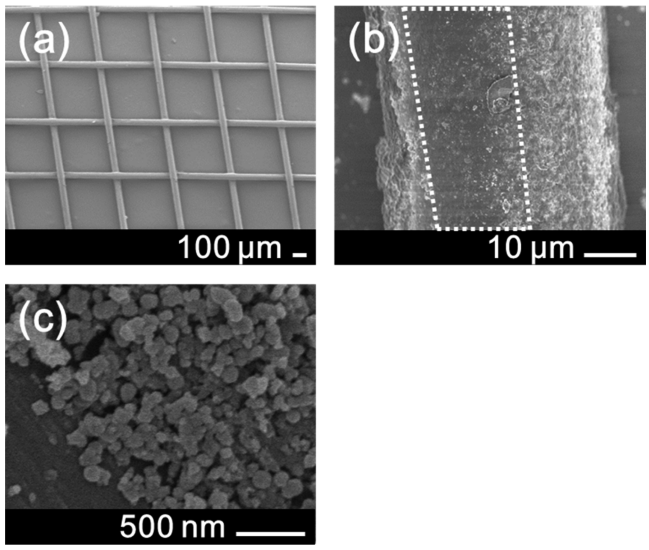

Figure 5. FE-SEM images of (a) the superhydrophobic polyester meshes after 100 cycles of abrasion with a pressure of ~10 kPa, (b) a higher magnification of a fiber in (a), and (c) the SiO_2 nanoparticles modified with PFOTS on a residual layer of (b).

Table 2. Water Contact Angles and Sliding Angles with and without PFDTS Treatment before and after 100 Cycles of Abrasion

	contact angle (deg)		sliding angle (deg)	
	before	after	before	after
with PFDTS treatment	153.2 ± 2.5	152.3 ± 2.3	11.1 ± 2.5	24.1 ± 1.5
without PFDTS treatment	154.6 ± 3.6	145.6 ± 5.9	11.2 ± 2.6	39.3 ± 3.8

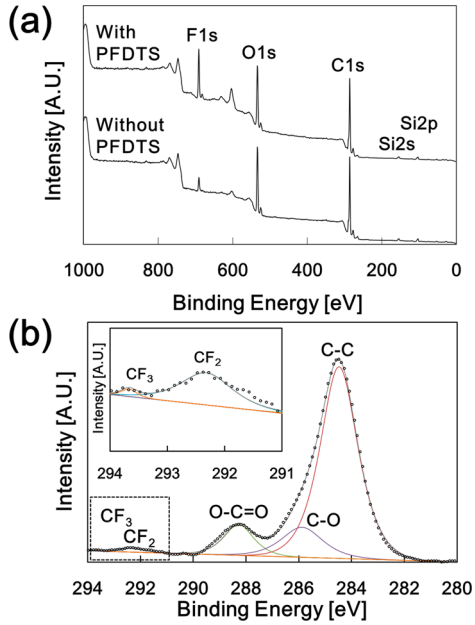

Figure 6. XPS spectra of the polyester surfaces with and without PFDTS treatment after 100 cycles of abrasion: (a) XPS survey spectra; (b) XPS core level spectra of the C 1s peaks.

spectra acquired from the surfaces with PFDTS treatment after abrasion, resolved into five components, namely, CF_3 (293.6

DOI: 10.1021/am508726k
ACS Appl. Mater. Interfaces 2015, 7, 4809−4816

Table 3. Surface Composition of the Polyester Surfaces with and without PFDTS Treatment after Abrasion from XPS Analyses

	%C	%O	%F	%Si	F/O
with PFDTS treatment	53.6	22.0	17.8	6.5	0.81
without PFDTS treatment	55.1	23.5	14.2	7.1	0.61

eV), CF_2 (292.3 eV), O−C═O (288.2 eV), C−O (285.9 eV), and C−C (284.5 eV). The intensity of the F 1s peak in the mesh treated with PFDTS is higher than that of the mesh without PFDTS treatment, while the peak intensities of the rest of the elements remain relatively unchanged, which implies that the polyester surface with the PFDTS treatment is covered with F (Figure 6a and Figure S2 of the Supporting Information). Therefore, even if the SiO_2 nanoparticles modified with PFOTS are removed by the abrasion, the mesh surfaces treated with PFDTS maintain their low surface energy property and retain their superhydrophobicity and low WSA. This concept is illustrated in Figure 7.

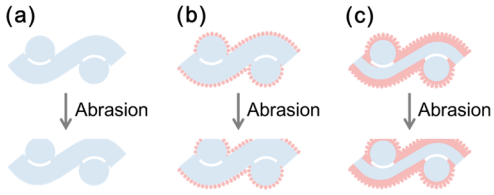

Figure 7. Effect of wear upon a surface with topography for the (a) pristine polyester mesh surface and (b) superhydrophobic surface without PFDTS treatment and (c) with PFDTS treatment.

Additionally, the contact angles and sliding angles of acidic and basic aqueous solutions with pH values from 2 to 14 are measured (Figure 8). All solution contact angles exceed 150° with sliding angles not beyond 15°, which indicates a good resistance to acidic and basic media.

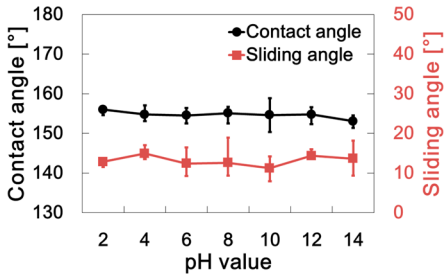

Figure 8. Contact angle and sliding angle measurements of the superhydrophobic meshes using aqueous solutions with a pH range of 2−14.

Transparency of the Fabricated Mesh. These superhydrophobic meshes are highly transparent, as is verified by UV−vis transmittance spectra (Figure 9), where the transmittance of the fabricated superhydrophobic mesh is approximately 80% in the spectral range of 400−1000 nm and possesses a maximum transmittance of 81.2%. The transmittance remains at approximately 79% in the spectral range 400−1000 nm and with a maximum transmittance of 80.2% after 100 cycles of abrasion under about 10 kPa of pressure. These results indicate that the coated meshes can withstand 100 abrasion cycles without a significant reduction in

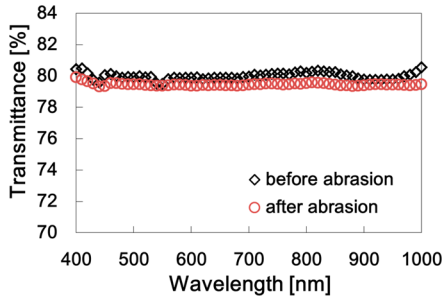

Figure 9. Ultraviolet−visible transmittance spectra of the superhydrophobic surfaces before and after 100 cycles of abrasion.

transparency. For the see-through structures of the original mesh, the transmittance is almost equal to the aperture ratio of the fabrics, so the transmittance of the mesh is almost constant in value for the spectral range of 400−1000 nm (Figure S3 of the Supporting Information). This transparency is reflected by the easy readability of the character underneath the coated mesh, and the superhydrophobicity of the mesh is demonstrated by the high contact angle of the blue-colored water droplets in Figure 10.

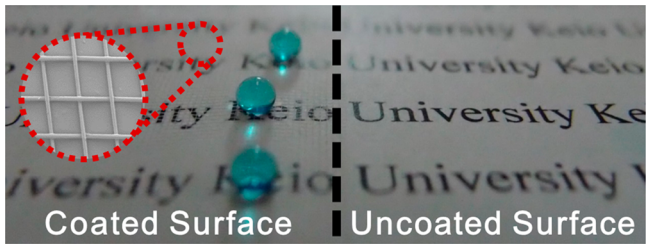

Figure 10. Photograph of blue-colored water on the coated polyester mesh surface (left) and a photograph of an uncoated surface on white paper for comparison.

Oil−Water Separation. To evaluate the oil wettability of the superhydrophobic mesh, we drop an *n*-octane droplet on the fabricated mesh surface, whereupon the *n*-octane droplet spreads through the mesh instantly upon contacting the substrate (Figure 11a and Movie S1of the Supporting Information). This demonstrates the oleophilic property of the mesh, which may be due to the large pore size of the mesh and the low surface tension of the *n*-octane droplet. In the case of water, however, the water droplet does not spread through the fabricated mesh but rebounds several times before undergoing damped oscillations and, finally, rests on the surface in the Cassie state (Figure 11b and Movie S2 of the Supporting Information). With the combination of superhydrophobicity and oleophilicity in the substrate, this mesh may be used for oil/water separation.

To evaluate the possibility of a functional mesh to separate oil from water, we design the simple oil/water separation setup shown in Figure 12a. The fabricated mesh is placed in a clamp with a tube on both sides. Because the mesh is almost transparent, the character picture pattern can be seen from the opposite side (Figure 12a inset). We then mix the dyed water and *n*-octane where, owing to its lower density, the oil remains above the water (Figure 12a). When the mixture of water and *n*-octane is poured into the feed inset, the oil/water mixture is separated successfully because of the superhydrophobic and oleophilic behavior of the mesh, wherein the water remains on

DOI: 10.1021/am508726k
ACS Appl. Mater. Interfaces 2015, 7, 4809−4816

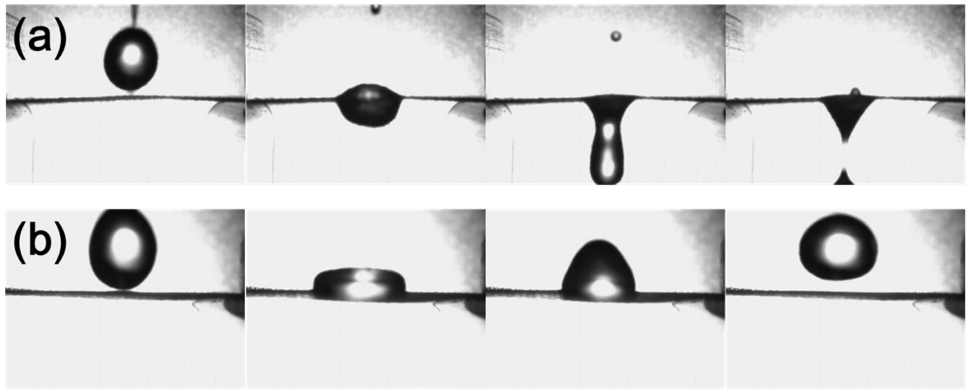

Figure 11. Superhydrophobicity and oleophilicity of the coated surface demonstrated by time-resolved images of (a) the wetting process of an *n*-octane droplet on the coated mesh and (b) the bouncing of a water droplet on the fabricated mesh.

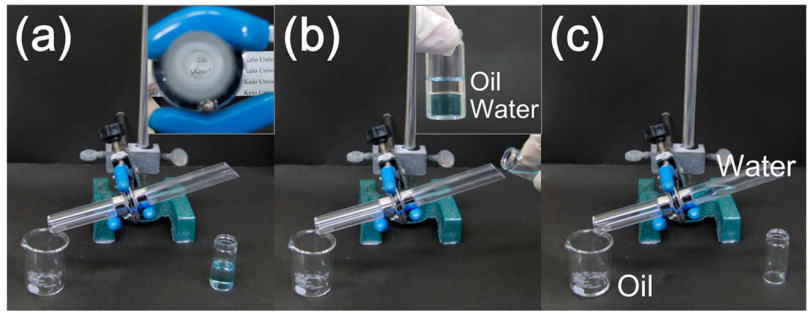

Figure 12. Oil/water separation studies of the coated mesh. Photographs of the (a) simple instrument fabricated for this study and (b) before and (c) after separation of the mixture of *n*-octane and blue-colored water.

the superhydrophobic mesh while the oil penetrates the mesh and flows down (Figure 12b and 12c). This oil/water separation can be conducted continuously, which indicates that the fabricated mesh maintains superhydrophobicity even after being wetted by *n*-octane.

CONCLUSIONS

A superhydrophobic polyester mesh possessing both mechanical stability and high transparency in the visible light range is fabricated by coating the PFDTS-treated fibers, after chemical etching, with SiO_2 nanoparticles modified with PFOTS. It is found that the fabricated mesh maintains its superhydrophobicity and low water sliding angle because of the PFDTS surface treatment, although the SiO_2 nanoparticles modified with PFOTS are removed by the abrasion. The vacant space between the mesh fibers allows the penetration of visible light and protects the nanoroughness provided by the SiO_2 nanoparticles; thus, it is unnecessary to control the refractive index of the materials for improving transparency and to contain strong chemical or physical bonding between the particles or the particles and the substrate for improving the abrasion resistance. Therefore, compared with the traditional technology, the combination of the see-through mesh and the SiO_2 nanoparticle hierarchical structure is an effective and simple method for improving the abrasion resistance and transparency of these superhydrophobic films. This simple but novel and effective method may be useful for the improvement of highly transparent superhydrophobic surfaces for various applications.

ASSOCIATED CONTENT

Supporting Information

FE-SEM images of the polyester meshes after alkaline treatment with NaOH (higher magnification images of the fibers in Figure 2); EDX images of the superhydrophobic polyester meshes after 100 cycles of abrasion; UV−vis spectra of the polyester meshes before and after alkaline treatment with NaOH at 75 and 80 °C for 120, 180, and 240 min; movies showing the superhydrophobic and oleophilic properties of the coated surface. This material is available free of charge via the Internet at http://pubs.acs.org.

AUTHOR INFORMATION

Corresponding Author

*E-mail: shiratori@appi.keio.ac.jp.

Author Contributions

N.Y. conceived, designed, and carried out the experiments, analyzed the data, and wrote the paper. S.S., K.M., and M.T. gave scientific advice and commented on the manuscript.

Notes

The authors declare no competing financial interest.

ACKNOWLEDGMENTS

We are deeply grateful to Mr. Shingo Nishizawa, whose comments and suggestions were immeasurably valuable throughout our study. We are indebted to Dr. Kouji Fujimoto, Dr. Kyu-Hong Kyung, and Dr. Yoshio Hotta, whose meticulous comments were an enormous help.

DOI: 10.1021/am508726k
ACS Appl. Mater. Interfaces 2015, 7, 4809−4816

REFERENCES

(1) Neinhuis, C.; Barthlott, W. Characterization and Distribution of Water-Repellent, Self-Cleaning Plant Surfaces. *Ann. Bot.* **1997**, *79*, 667−677.

(2) Shirtcliffe, N. J.; Pyatt, F. B.; Newton, M. I.; McHale, G. A Lichen Protected by a Super-Hydrophobic and Breathable Structure. *J. Plant Physiol.* **2006**, *163*, 1193−1197.

(3) Koch, K.; Bhushan, B.; Barthlott, W. Multifunctional Surface Structures of Plants: An Inspiration for Biomimetics. *Prog. Mater. Sci.* **2009**, *54*, 137−178.

(4) Gao, X. F.; Jiang, L. Water-Repellent Legs of Water Striders. *Nature* **2004**, *432*, 36.

(5) Bai, F.; Wu, J.; Gong, G.; Guo, L. Biomimetic Water Strider Leg with Highly Refined Nanogroove Structure and Remarkable Water-Repellent Performance. *ACS Appl. Mater. Interfaces* **2014**, *6*, 16237−16242.

(6) Hansen, W. R.; Autumn, K. Evidence for Self-Cleaning in Gecko Setae. *Proc. Natl. Acad. Sci. U. S. A.* **2005**, *102*, 385−389.

(7) Lee, W.; Jin, M. K.; Yoo, W. C.; Lee, J. K. Nanostructuring of a Polymeric Substrate with Well-Defined Nanometer-Scale Topography and Tailored Surface Wettability. *Langmuir* **2004**, *20*, 7665−7669.

(8) Wenzel, R. N. Resistance of Solid Surfaces to Wetting by Water. *Ind. Eng. Chem.* **1936**, *28*, 988−994.

(9) Cassie, A.; Baxter, S. Wettability of Porous Surfaces. *Trans. Faraday Soc.* **1944**, *40*, 546−551.

(10) Extrand, C. W. Modeling of Ultralyophobicity: Suspension of Liquid Drops by a Single Asperity. *Langmuir* **2005**, *21*, 10370−10374.

(11) Gao, L. C.; McCarthy, T. J. The "Lotus Effect" Explained: Two Reasons Why Two Length Scales of Topography Are Important. *Langmuir* **2006**, *22*, 2966−2967.

(12) Nakajima, A.; Hashimoto, K.; Watanabe, T. Transparent Superhydrophobic Thin Films with Self-Cleaning Properties. *Langmuir* **2000**, *16*, 7044−7047.

(13) Onda, T.; Shibuichi, S.; Satoh, N.; Tsujii, K. Super-Water-Repellent Fractal Surfaces. *Langmuir* **1996**, *12*, 2125−2127.

(14) Guo, P.; Zheng, Y.; Liu, C.; Jub, J.; Jiang, L. Directional Shedding-Off of Water on Natural/Bio-mimetic Taper−Ratchet Array Surfaces. *Soft Matter* **2012**, *8*, 1770−1775.

(15) Liao, Y.; Loh, C. H.; Wang, R.; Fane, A. G. Electrospun Superhydrophobic Membranes with Unique Structures for Membrane Distillation. *ACS Appl. Mater. Interfaces* **2014**, *6*, 16035−16048.

(16) Xu, W.; Song, J.; Sun, J.; Lu, Y.; Yu, Z. Rapid Fabrication of Large-Area, Corrosion-Resistant Superhydrophobic Mg Alloy Surfaces. *ACS Appl. Mater. Interfaces* **2011**, *3*, 4404−4414.

(17) Liu, H.; Szunerits, S.; Xu, W.; Boukherroub, R. Preparation of Superhydrophobic Coatings on Zinc as Effective Corrosion Barriers. *ACS Appl. Mater. Interfaces* **2009**, *1*, 1150−1153.

(18) Liu, H.; Szunerits, S.; Pisarek, M.; Xu, W.; Boukherroub, R. Preparation of Superhydrophobic Coatings on Zinc, Silicon, and Steel by a Solution-Immersion Technique. *ACS Appl. Mater. Interfaces* **2009**, *1*, 2086−2091.

(19) Verplanck, N.; Coffinier, Y.; Thomy, V.; Boukherroub, R. Wettability Switching Techniques on Superhydrophobic Surfaces. *Nanoscale Res. Lett.* **2007**, *2*, 577−596.

(20) Solga, A.; Cerman, Z.; Striffler, B. F.; Spaeth, M.; Barthlott, W. The Dream of Staying Clean: Lotus and Biomimetic Surfaces. *Bioinspiration Biomimetics* **2007**, *2*, 126−134.

(21) Gao, L.; McCarthy, T. J. "Artificial Lotus Leaf" Prepared Using a 1945 Patent and a Commercial Textile. *Langmuir* **2006**, *22*, 5998−6000.

(22) Choi, W.; Tuteja, A.; Chhatre, S.; Mabry, J. M.; Cohen, R. E.; McKinley, G. H. Fabrics with Tunable Oleophobicity. *Adv. Mater.* **2009**, *21*, 2190−2195.

(23) Deng, B.; Cai, R.; Yu, Y.; Jiang, H.; Wang, C.; Li, J.; Li, L.; Yu, M.; Li, J.; Xie, L.; Huang, Q.; Fan, C. Laundering Durability of Superhydrophobic Cotton Fabric. *Adv. Mater.* **2010**, *22*, 5473−5477.

(24) Gao, X.; Yan, X.; Yao, X.; Xu, L.; Zhang, K.; Zhang, J.; Yang, B.; Jiang, L. The Dry-Style Antifogging Properties of Mosquito Compound Eyes and Artificial Analogues Prepared by Soft Lithography. *Adv. Mater.* **2007**, *19*, 2213−2217.

(25) Cao, L.; Jones, A.; Sikka, V.; Wu, J. Anti-Icing Superhydrophobic Coatings. *Langmuir* **2009**, *25*, 12444−12448.

(26) Xu, Q.; Li, J.; Tian, J.; Zhu, J.; Gao, X. Energy-Effective Frost-Free Coatings Based on Superhydrophobic Aligned Nanocones. *ACS Appl. Mater. Interfaces* **2014**, *6*, 8976−8980.

(27) Davis, A.; Yeong, Y. H.; Steele, A.; Bayer, I. S.; Loth, E. Superhydrophobic Nanocomposite Surface Topography and Ice Adhesion. *ACS Appl. Mater. Interfaces* **2014**, *6*, 9272−9279.

(28) Pan, Q.; Wang, M. Miniature Boats with Striking Loading Capacity Fabricated from Superhydrophobic Copper Meshes. *ACS Appl. Mater. Interfaces* **2009**, *1*, 420−423.

(29) Ou, J.; Perot, B.; Rothstein, J. P. Laminar Drag Reduction in Microchannels Using Ultrahydrophobic Surfaces. *Phys. Fluids* **2004**, *16*, 4635−4643.

(30) Verho, T.; Bower, C.; Andrew, P.; Franssila, S.; Ikkala, O.; Ras, R. H. A. Mechanically Durable Superhydrophobic Surfaces. *Adv. Mater.* **2011**, *23*, 673−678.

(31) Artus, G. R. J.; Seeger, S. Scale-Up of a Reaction Chamber for Superhydrophobic Coatings Based on Silicone Nanofilaments. *Ind. Eng. Chem. Res.* **2012**, *51*, 2631−2636.

(32) Peng, S.; Yang, X.; Tian, D.; Deng, W. Chemically Stable and Mechanically Durable Superamphiphobic Aluminum Surface with a Micro/Nanoscale Binary Structure. *ACS Appl. Mater. Interfaces* **2014**, *6*, 15188−15197.

(33) Xu, L.; Geng, Z.; He, J.; Zhou, G. Mechanically Robust, Thermally Stable, Broadband Antireflective, and Superhydrophobic Thin Films on Glass Substrates. *ACS Appl. Mater. Interfaces* **2014**, *6*, 9029−9035.

(34) Zhang, X.; Guo, Y.; Zhang, Z.; Zhang, P. Facile Approach for Preparation of Stable Water-Repellent Nanoparticle Coating. *Appl. Surf. Sci.* **2012**, *258*, 7907−7911.

(35) Wang, H.; Xue, Y.; Ding, J.; Feng, L.; Wang, X.; Lin, T. Durable, Self-Healing Superhydrophobic and Superoleophobic Surfaces from Fluorinated-Decyl Polyhedral Oligomeric Silsesquioxane and Hydrolyzed Fluorinated Alkyl Silane. *Angew. Chem., Int. Ed.* **2011**, *50*, 11433−11436.

(36) Shchukin, D. G.; Möhwald, H. Self-Repairing Coatings Containing Active Nanoreservoirs. *Small* **2007**, *3*, 926−943.

(37) Dikíc, T.; Ming, W.; van Benthem, R. A. T. M.; Esteves, A. C. C.; de With, G. Self-Replenishing Surfaces. *Adv. Mater.* **2012**, *24*, 3701−3704.

(38) Xu, L.; Karunakaran, R. G.; Guo, J.; Yang, S. Transparent, Superhydrophobic Surfaces from One-Step Spin Coating of Hydrophobic Nanoparticles. *ACS Appl. Mater. Interface* **2012**, *4*, 1118−1125.

(39) Deng, X.; Mammen, L.; Butt, H. J.; Vollmer, D. Candle Soot as a Template for a Transparent Robust Superamphiphobic Coating. *Science* **2012**, *335*, 67−70.

(40) Du, X.; Li, X.; He, J. Facile Fabrication of Hierarchically Structured Silica Coatings from Hierarchically Mesoporous Silica Nanoparticles and Their Excellent Superhydrophilicity and Superhydrophobicity. *ACS Appl. Mater. Interfaces* **2010**, *2*, 2365−2372.

(41) Wang, D.; Zhang, Z.; Li, Y.; Xu, C. Highly Transparent and Durable Superhydrophobic Hybrid Nanoporous Coatings Fabricated from Polysiloxane. *ACS Appl. Mater. Interfaces* **2014**, *6*, 10014−10021.

(42) Manabe, K.; Nishizawa, S.; Kyung, K. H.; Shiratori, S. Optical Phenomena and Antifrosting Property on Biomimetics Slippery Fluid-Infused Antireflective Films via Layer-by-Layer Comparison with Superhydrophobic and Antireflective Films. *ACS Appl. Mater. Interfaces* **2014**, *6*, 13985−13993.

(43) Yanagisawa, T.; Nakajima, A.; Sakai, M.; Kameshima, Y.; Okada, K. Preparation and Abrasion Resistance of Transparent Superhydrophobic Coating by Combining Crater-Like Silica Films with Acicular Boehmite Powder. *Mater. Sci. Eng. B* **2009**, *161*, 36−39.

(44) Nishizawa, S.; Shiratori, S. Fabrication of Semi-Transparent Superoleophobic Thin Film by Nanoparticle-Based Nano−Microstructures on See-Through Fabrics. *J. Mater. Sci.* **2013**, *48*, 6613−6618.

DOI: 10.1021/am508726k
ACS Appl. Mater. Interfaces 2015, 7, 4809−4816

(45) Wang, L.; Zhang, X.; Li, B.; Sun, P.; Yang, J.; Xu, H.; Liu, Y. Superhydrophobic and Ultraviolet-Blocking Cotton Textiles. *ACS Appl. Mater. Interfaces* **2011**, *3*, 1277−1281.
(46) Xue, C. H.; Li, Y. R.; Zhang, P.; Ma, J. Z.; Jia, S. T. Washable and Wear-Resistant Superhydrophobic Surfaces with Self-Cleaning Property by Chemical Etching of Fibers and Hydrophobization. *ACS Appl. Mater. Interfaces* **2014**, *6*, 10153−10161.
(47) Liu, N.; Cao, Y.; Lin, X.; Chen, Y.; Feng, L.; Wei, Y. A Facile Solvent-Manipulated Mesh for Reversible Oil/Water Separation. *ACS Appl. Mater. Interfaces* **2014**, *6*, 12821−12826.
(48) Gondal, M. A.; Sadullah, M. S.; Dastageer, M. A.; McKinley, G. H.; Panchanathan, D.; Varanasi, K. K. Study of Factors Governing Oil−Water Separation Process Using TiO_2 Films Prepared by Spray Deposition of Nanoparticle Dispersions. *ACS Appl. Mater. Interfaces* **2014**, *6*, 13422−13429.
(49) Lee, C. H.; Johnson, N.; Drelich, J.; Yap, Y. K. The Performance of Superhydrophobic and Superoleophilic Carbon Nanotube Meshes in Water−Oil Filtration. *Carbon* **2011**, *49*, 669−676.
(50) Gu, J.; Xiao, P.; Chen, J.; Zhang, J.; Huang, Y.; Chen, T. Janus Polymer/Carbon Nanotube Hybrid Membranes for Oil/Water Separation. *ACS Appl. Mater. Interfaces* **2014**, *6*, 16204−16209.
(51) Fakhru'l-Razi, A.; Pendashteh, A.; Abdullah, L. C.; Biak, D. R. A.; Madaeni, S. S.; Abidin, Z. Z. Review of Technologies for Oil and Gas Produced Water Treatment. *J. Hazard. Mater.* **2009**, *170*, 530−551.
(52) Zhang, X.; Guo, Y.; Zhang, P.; Wu, Z.; Zhang, Z. Superhydrophobic and Superoleophilic Nanoparticle Film: Synthesis and Reversible Wettability Switching Behavior. *ACS Appl. Mater. Interfaces* **2012**, *4*, 1742−1746.
(53) Xue, C. H.; Zhang, P.; Ma, J. Z.; Ji, P. T.; Li, Y. R.; Jia, S. T. Long-Lived Superhydrophobic Colorful Surfaces. *Chem. Commun.* **2013**, *49*, 3588−3590.
(54) Song, X. Y.; Zhai, J.; Wang, Y. L.; Jiang, L. Fabrication of Superhydrophobic Surfaces by Self-Assembly and Their Water-Adhesion Properties. *J. Phys. Chem. B* **2005**, *109*, 4048−4052.
(55) Tejimbayashi, M.; Shiratori, S. Highly Durable Superhydrophobic Coatings with Gradient Density by Movable Spray Method. *J. Appl. Phys.* **2014**, *116*, 114310.
(56) Collins, M. J.; Zeronian, S. H.; Semmelmeyer, M. The Use of Aqueous Alkaline Hydrolysis To Reveal the Fine Structure of Poly(ethylene terephthalate) Fibers. *J. Appl. Polym. Sci.* **1991**, *42*, 2149−2162.

DOI: 10.1021/am508726k
ACS Appl. Mater. Interfaces 2015, 7, 4809−4816